Computational Materials Today 1 (2024) 100002

Contents lists available at ScienceDirect

Computational Materials Today

journal homepage: www.sciencedirect.com/journal/computational-materials-today

Partially deorbitalized meta-GGA

P. Bonfà[a], S. Sharma[b,c], J.K. Dewhurst[d,*]

[a] Dipartimento di Scienze Matematiche, Fisiche e Informatiche, Università di Parma, I-43124 Parma, Italy
[b] Max-Born-Institute for Non-linear Optics and Short Pulse Spectroscopy, Berlin 12489, Germany
[c] Institute for Theoretical Solid-state Physics, Arnimallee 14, Berlin 14195, Germany
[d] Max-Planck-Institut für Mikrostrukturphysik, Weinberg 2, Halle D-06120, Germany

A B S T R A C T

Mejia-Rodriguez and Trickey recently proposed a procedure for removing the explicit dependence of meta-GGA exchange-correlation energy functionals E_{xc} on the kinetic energy density τ. We present a simple modification to this approach in which the exact Kohn-Sham τ is used as input for E_{xc} but the functional derivative of τ with respect to the density ρ, required to calculate the potential term $\int d^3r' \, \delta E_{xc}/\delta\tau(\mathbf{r}')|_\rho \cdot \delta\tau(\mathbf{r}')/\delta\rho(\mathbf{r})$, is evaluated using an approximate kinetic energy density functional. This 'half-way' strategy ensures that the Kohn-Sham potential is a local multiplicative function (as opposed to the non-local potential of a generalized Kohn-Sham approach) while preserving the inherent non-locality of the functional itself. Electronic structure codes can be easily modified to use the new method. We validate it by quantifying the accuracy of the predicted lattice parameters, bulk moduli, magnetic moments and cohesive energies of a large set of periodic solids. An unanticipated benefit of this method is to gauge the quality of approximate kinetic energy functionals by checking if the self-consistent solution is indeed at the variational minimum.

1. Introduction

The exchange-correlation energy functional, E_{xc}, is an essential component of the Kohn-Sham (KS) [1] formulation of density functional theory (DFT) [2]. Knowledge of E_{xc} allows for both the exact electronic density and the total energy of a system of interacting electrons in an external potential to be determined. In practice however, E_{xc} has to be approximated, the inevitable result of which is inexact densities and energies. Consequently, much effort has been expended over that past several decades on inventing ever more sophisticated approximations.

The simplest approximation for the unknown exchange and correlation functional is the Local Density Approximation (LDA), in which the functional is supposed to depend locally on the charge density. LDA represents the zeroth order expansion of E_{xc} in terms of electron density gradients and constitutes the first rung of the so-called 'Jacob's ladder' of density functional approximations [3]. On the second rung, the Generalized Gradient Approximation (GGA), takes into account density gradients [4], and satisfies more known properties of the exact functional. However, because of the limitations of a semi-local functional form, GGAs tend to be accurate for either energies or equilibrium geometries, but not both [5]. The third rung of functionals, meta-GGAs, were conceived to address this limitation by including the Kohn-Sham kinetic energy (KE) density explicitly in their formulation [6–8]. This choice originates with Becke [9] who found that the KE density emerged naturally in an gradient expansion of the exchange charge density. Meta-GGA functionals are truly non-local because of the implicit orbital dependence of the KE density on the density itself. This additional flexibility also allows for more known exact conditions to be satisfied. In fact, the strongly constrained and appropriately normalized (SCAN) functional [10,11] satisfies all 17 known exact conditions that a meta-GGA can.

For the spin unpolarized case, the meta-GGA exchange-correlation energy is given by

$$E_{xc}[\rho, \tau] = \int d^3r \, \epsilon_{xc}(\rho(\mathbf{r}), |\nabla\rho(\mathbf{r})|, \tau(\mathbf{r}))\rho(\mathbf{r}),$$

where

$$\rho(\mathbf{r}) \equiv \sum_{i=1}^{N} |\varphi_i(\mathbf{r})|^2 \tag{1}$$

is the density and

$$\tau(\mathbf{r}) \equiv \frac{1}{2}\sum_{i=1}^{N} |\nabla\varphi_i(\mathbf{r})|^2 \tag{2}$$

is the non-interacting, Kohn-Sham KE density, with φ_i being the ith Kohn-Sham orbital of a state with N electrons. For its intended use, the KE density is not an independent variable but rather an implicit functional of the density, i.e. $\tau(\mathbf{r}) \equiv \tau[\rho](\mathbf{r})$. This functional dependence is not arbitrary but means: "τ is the KE density of that Kohn-Sham system which reproduces ρ". However, this dependency is rarely satisfied in

* Corresponding author.
E-mail address: dewhurst@mpi-halle.mpg.de (J.K. Dewhurst).

https://doi.org/10.1016/j.commt.2024.100002
Received 25 January 2024; Received in revised form 25 March 2024; Accepted 29 March 2024
Available online 1 April 2024

practice because of the difficulty that arises when one has to determine the exchange-correlation potential $v_{\rm xc}$ as the functional derivative of $E_{\rm xc}$ with respect to the density:

$$v_{\rm xc}(\mathbf{r}) = \frac{\delta E_{\rm xc}[\rho,\,\tau]}{\delta\rho(\mathbf{r})}\bigg|_{\tau} + \int d^3r' \frac{\delta E_{\rm xc}[\rho,\,\tau]}{\delta\tau(\mathbf{r}')}\bigg|_{\rho} \frac{\delta\tau(\mathbf{r}')}{\delta\rho(\mathbf{r})}. \tag{3}$$

The last term requires the functional derivative of τ with respect to ρ. This is numerically difficult to perform and involves an approach similar to that used for the optimized effective potential (OEP) method [12]. Instead, codes typically calculate potentials determined from the derivative with respect to the orbitals $\delta E_{\rm xc}/\delta\varphi(\mathbf{r})$. Such an approach, however, produces a non-local potential [13] and is referred to as *generalized* Kohn-Sham (gKS), although this terminology is fairly broad. For example, a version of gKS was defined exactly by Garrick, *et al.* [14] and requires adding a specified fraction of Fock exchange. This is intended to justify certain types of hybrid functionals, but is clearly not applicable to the gKS used with meta-GGA. A more relevant approach is to extend the defintion of DFT to include the *exact* kinetic-energy density (i.e. that of the fully interacting system) as a genuinely independent variable, and demand that the Kohn-Sham system reproduce both ρ and τ; see Theophilou, *et al.* [15]. Nevertheless, this is not the intended use of SCAN and other meta-GGAs which are strictly density-only functionals.

Thus we have a dilemma: the great intellectual effort expended to satisfy as many exact constraints as possible is undermined by violating a fundamental property of the KS potential, namely that it be a local function in **r**. Yet the choice of τ by the inventors of meta-GGA forces the writers of electronic structure codes to have to deal with the difficult functional derivative, or avoid it altogether with gKS. A practical consequence of this is the inability to fairly judge the performance of meta-GGA functionals against their antecedents. For instance, one cannot say definitively whether a particular meta-GGA functional is better than a particular GGA if there is an error introduced by evaluating the meta-GGA functional with gKS.

Mejía-Rodríguez and Trickey (MRT) neatly sidestepped this problem by replacing the τ determined from the orbitals via Eq. (2) with one obtained from an approximate KE density functional [16–18]. This 'deorbitalized' meta-GGA was found to produce results of accuracy which were comparable to that of the gKS method. This approach however, removes the true non-locality of $E_{\rm xc}$ and in effect reduces meta-GGA to a semi-local GGA-like functional (albeit possibly with Laplacian terms [19]). Notably, this is not the first attempt to produce an orbital-free meta-GGA functional and approaches based on the Laplacian of the density [20] or other parameters such as the density overlap regions indicator [21,22] have been previously proposed in literature.

In the current work we adopt a 'half-way' strategy, in that we use the KS orbital-derived τ as *input* to the functional, but use an approximate KE density functional to evaluate *only the functional derivative* in Eq. (3). We term this approach 'partial deorbitalization' (PD) and find that even a fairly primitive KE functional, like the Thomas-Fermi-von Weizsäcker (TFvW) gradient expansion [23], yields accurate results. This deorbitalization scheme can be easily implemented in codes which already employ the generalized Kohn-Sham version of meta-GGA. Partial deorbitalization retains the 'exact' τ for the energy but utilizes both the exact and approximate τ for the potential, which favors situations in which the main error is functional-driven rather than density-driven [24].

The self-consistent density determined in this way will not be strictly variational, i.e. it may not equal to the lowest energy solution. In fact, this will be demonstrated for the magnetic case later in the article. The absence of a variational solution is not as great an encumbrance as one may imagine: the WIEN2k code, for example, evaluates the energy of meta-GGA functionals with densities computed with GGA [25]. Likewise, potential-only functionals like Becke-Johnson [26] or Tran-Blaha [27] are not the variational minimum of a given energy functional. Our approach at least has the possibility of being variational if the exact functional derivative is employed. However, as we show in the Supplemental Material (SM), even using a fairly simple KE functional such as TFvW, the atomic forces are acceptably close to the gradient of the total energy.

All these approaches have their drawbacks: gKS because it treats ρ and τ as independent variables; deorbitalized meta-GGA because τ is calculated exclusively with an approximate KE density functional; and partial deorbitalization because it is not variational. If, however, we are committed to the principle of satisfying as many known exact constraints of DFT as possible, then we should insist that $v_{\rm xc}$ be local in **r**. By continuing to improve the approximations to both $E_{\rm xc}$ and τ, there is no fundamental impediment on the path to exact Kohn-Sham via partial deorbitalization.

2. Approximations

As will be demonstrated later, the method does not require a particularly sophisticated KE density functional for calculating the functional derivative $\delta\tau(\mathbf{r}')/\delta\rho(\mathbf{r})$ in Eq. (3). Here we choose to use the gradient expansion of τ with the TFvW terms [23] for the sake of ease of implementation:

$$\tilde{\tau}(\rho(\mathbf{r}),\,\sigma(\mathbf{r})) = \frac{3}{10}(3\pi^2)^{2/3}\rho^{5/3}(\mathbf{r}) + \frac{1}{72}\frac{\sigma(\mathbf{r})}{\rho(\mathbf{r})}, \tag{4}$$

where $\sigma(\mathbf{r}) \equiv |\nabla\rho(\mathbf{r})|^2$. In this case, the second term in Eq. (3) becomes

$$\int d^3r'\, w_{\rm xc}(\mathbf{r}')\frac{\delta\tilde{\tau}(\mathbf{r}')}{\delta\rho(\mathbf{r})} = w_{\rm xc}(\mathbf{r})\frac{\partial\tilde{\tau}(\mathbf{r})}{\partial\rho(\mathbf{r})}\bigg|_{\sigma} - 2\nabla\cdot\left[w_{\rm xc}(\mathbf{r})\frac{\partial\tilde{\tau}(\mathbf{r})}{\partial\sigma(\mathbf{r})}\bigg|_{\rho}\nabla\rho(\mathbf{r})\right],$$

where $w_{\rm xc}(\mathbf{r}) \equiv \delta E_{\rm xc}/\delta\tau(\mathbf{r})|_{\rho}$.

The spin polarized case is a straight-forward extension to the unpolarized case: the meta-GGA functional is generalized to the collinear form

$$E_{\rm xc}[\rho^{\uparrow},\,\rho^{\downarrow},\,\tau^{\uparrow},\,\tau^{\downarrow}] = \int d^3r\; \epsilon_{\rm xc}(\rho^{\uparrow}(\mathbf{r}),\,\rho^{\downarrow}(\mathbf{r}),\,\tau^{\uparrow}(\mathbf{r}),\,\tau^{\downarrow}(\mathbf{r}))\rho(\mathbf{r}),$$

where $\rho^{\uparrow\downarrow}$ and $\tau^{\uparrow\downarrow}$ are the up- and down-spin density and KE density, respectively. The total Kohn-Sham KE satisfies [28]

$$T_s[\rho^{\uparrow},\,\rho^{\downarrow}] = \frac{1}{2}T_s[2\rho^{\uparrow}] + \frac{1}{2}T_s[2\rho^{\downarrow}],$$

thus we will take spin-up KE density to depend exclusively on the spin-up density [19], $\tau^{\uparrow}[\rho^{\uparrow},\,\rho^{\downarrow}](\mathbf{r}) \equiv \tau^{\uparrow}[\rho^{\uparrow}](\mathbf{r})$, and likewise for the spin-down density. This implies that $\delta\tau^{\uparrow}(\mathbf{r}')/\delta\rho^{\downarrow}(\mathbf{r})|_{\rho^{\uparrow}} = \delta\tau^{\downarrow}(\mathbf{r}')/\delta\rho^{\uparrow}(\mathbf{r})|_{\rho^{\downarrow}} = 0$. The spin-up exchange-correlation potential, for example, is then given by

$$v^{\uparrow}_{\rm xc}(\mathbf{r}) = \frac{\delta E_{\rm xc}}{\delta\rho^{\uparrow}(\mathbf{r})}\bigg|_{\rho^{\downarrow},\tau^{\uparrow},\tau^{\downarrow}} + \int d^3r' \frac{\delta E_{\rm xc}}{\delta\tau^{\uparrow}(\mathbf{r}')}\bigg|_{\rho^{\uparrow},\rho^{\downarrow},\tau^{\downarrow}} \frac{\delta\tau^{\uparrow}(\mathbf{r}')}{\delta\rho^{\uparrow}(\mathbf{r})},$$

which can be easily approximated for the spin-polarized TFvW KE density

$$\tilde{\tau}^{\uparrow}(\rho^{\uparrow}(\mathbf{r}),\,\sigma^{\uparrow}(\mathbf{r})) = \frac{1}{2}\tilde{\tau}(2\rho^{\uparrow}(\mathbf{r}),\,4\sigma^{\uparrow}(\mathbf{r})),$$

where $\sigma^{\uparrow}(\mathbf{r}) = |\nabla\rho^{\uparrow}(\mathbf{r})|^2$.

3. Computational Details

The goal of the following section is to evaluate the accuracy of our partial deorbitalization strategy. We do so by validating its *ab initio* predictions against a large number of experimental results. We also list in the SM the computational outcomes of the previous work by MRT [18], including both the results from their gKS and the fully deorbitalized meta-GGA simulations based on the r2SCAN [29,30] functional, in order to compare against different strategies for deorbitalizing meta-GGA. In the following, the results of MRT obtained with the plane-wave based code VASP [31,32], PAW pseudopotentials [33], and the r2SCAN

exchange and correlation functional[1] will be referred to as gKS. The label FD will indicate "full deorbitalization" and in the present case refers to the r2SCAN-L functional. The partially deorbitalized r2SCAN meta-GGA results are instead labelled PD.

In order to compute equilibrium lattice parameters and bulk moduli with high accuracy, we opt for a Full Potential (FP) description of the electronic wave-functions with an APW basis [34]. This choice is effective for periodic systems but makes it difficult to compute the total energy of isolated atoms owing to the growing number of plane-waves required to describe the empty space between the atoms in the progressively larger supercells needed to suppress periodic image effects. To overcome this problem, we also use a plane-wave basis set and pseudopotentials for the estimation of the cohesive energies, where the adoption of iterative diagonalization makes convergence possible.

The Elk code [35] version 9.2.1 is used to perform FP simulations. Reciprocal space sampling is performed with at least a 17 × 17 × 17 Monkhorst-Pack grid. The basis is expanded up to $R_{MT}|\mathbf{G}+\mathbf{k}|_{\max} \geq 7$. The remaining parameters are set by the `highq` option.

For plane-wave simulations we use the Quantum ESPRESSO package [36] and opt for norm-conserving pseudopotentials [37] generated with the PBE [4] exchange and correlation functional. The reciprocal space sampling and the cut-off energy for the KS wavefunction expansion have been converged in order to obtain better than 1 mRy/atom accuracy in the total energy.

Estimation of atomic energies with meta-GGA requires further care. The exponentially vanishing charge produces a problematic behavior in the exchange and correlation potential across the self consistent cycles. There are two options to improve the convergence. The first is to converge isolated atom simulations with GGA (we used PBE) and later reuse the converged electronic charge as the starting point of meta-GGA simulations (for both gKS and PD). The alternative method consists of introducing a cut-off for vanishing charge density that removes the ill-behaving contributions from the exchange and correlation potential. This parameter can be converged together with the remaining settings governing the basis expansion. Numerically equivalent results are obtained with both approaches, when convergence can be achieved. The details are reported in the SM.

Following MRT, the equilibrium lattice constants a_0 and bulk moduli B_0 at $T = 0$ K were determined by calculating the total energy per unit cell in the range $V_0 \pm 10\%$ (where V0 is the equilibrium unit cell volume), followed by a twenty point fit to the stabilized jellium equation of state (SJEOS) [17,38].

4. Results and discussion

The complete set of results obtained for the computation of the equilibrium lattice parameters of 45 solids is presented, together with statistical data analysis, in Fig. 1, where panels (a) and (b) report the absolute and relative deviations. All absolute values are reported in Table S1 of the SM. Values for gKS are taken from Ref. [18] while our results for FD and PD are shown in the second and third columns of the figure and in the fifth and sixth columns of the table. Finally, the reference experimental data are based on zero-point corrected experimental lattice constants, detailed in Ref. [40] and references therein.

FD and PD show similar trends and comparable agreement with respect to experimental lattice parameters. Alkali metals are a notable exception, where deviations by more than 2% are observed. This is indeed a known issue with the SCAN family of functionals that originates from a poor description of the semi-core region of these elements, as explained in detail in Ref. [41]. No clear indications of over-binding or under-binding can be identified when considering at the whole set. Yet we note that FD and PD show similar trends across the periodic table. The mean absolute deviation (MAD) is 0.032 Å, 0.033 Å and 0.036 Å for gKS, FD and PD respectively.

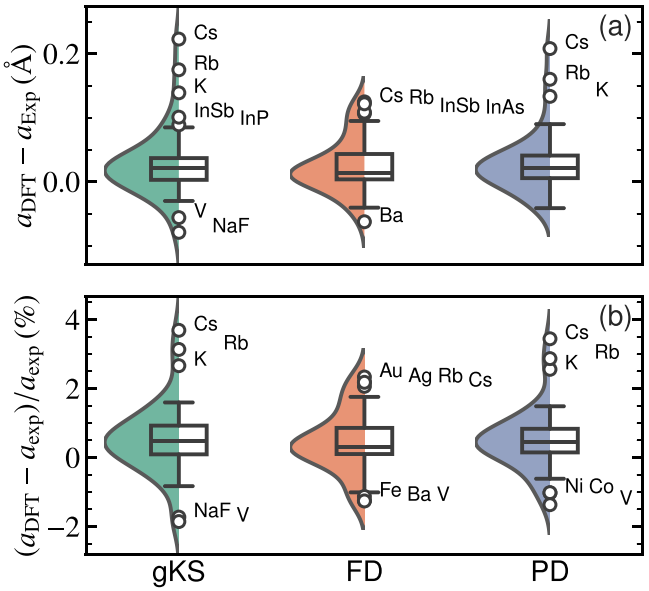

Fig. 1. Visualization (violin plot and box plot) of the deviations from experimental data of the predicted lattice parameter obtained with the different implementations of meta-GGA. The upper(lower) panel gives absolute(relative) deviations. The violin plots (transparent color) represent the data distribution and are based on a Gaussian kernel density estimation implemented in seaborn [39]. In the box plot, the boxes hold 50% of the data, with equal number of data points above and below the median deviation (full black line). The whiskers indicate the range of data falling within 1.5 × box-length beyond the upper and lower limits of the box (from the first quartile to the third quartile). The whiskers extend from the box by 1.5 × the inter-quartile range. Outliers beyond this range are indicated with circular makers and the solids' labels are reported on the right of each point.

The distribution of deviations is similar for the gKS, FD and PD schemes, but it is noted that almost the same outliers are found in the upper part of the box-plot for both gKS and PD meta-GGA, while additional outliers appear on both sides of the distributions of Fig. 1(b) for FD and PD.

Fig. 2 reports the same statistical analysis for the bulk moduli of 43 cubic systems.[2] All results are also tabulated in Table S2 of the SM and the experimental values are from Ref. [42,43]. The most significant discrepancies are observed also in this case for alkali metals. Additional outliers are found in transition metal elements, Cu and Au, and in wide-bandgap semiconductors (GaN and BN). The distribution of PD and gKS compare equally well against the experiment, while FD is showing slightly worse performance, as it can be appreciated from the box-plots of Fig. 2. The MAD for the bulk modulus is 6.1, 9.7 and 6.2 GPa for gKS, FD and PD respectively.

The Kohn-Sham (KS) band gaps for selected insulators and semiconductors are shown in Table 1. The results obtained with PD are similar to the ones produced by FD and in both cases the values are smaller than those obtained with gKS. This systematic difference is a well known property of the generalized KS theory and an accurate analysis of this point is presented in Ref. [45]. The results of FD and PD are instead obtained with a local potential and are therefore expected to match the previous results of the optimized effective potential reported in the last column of Table 1.

Cohesive energies are reported in Table 2 along with experimental atomization energies from Ref. [17,48,47]. As already mentioned, these results have been obtained with PW based simulations and in this case a larger discrepancy between the *ab initio* predictions and the experiment is observed, especially for transition metals. Notably, MRT results obtained with the gKS approach are in slightly better agreement than our gKS (first and third columns). This may be due to the adoption of norm

[1] A complete description of the methodological details is provided in the original reference.

[2] Fe and Co have been removed from the analysis to allow the comparison with Refs. [18] where the Bulk modulus for these compounds is not reported.

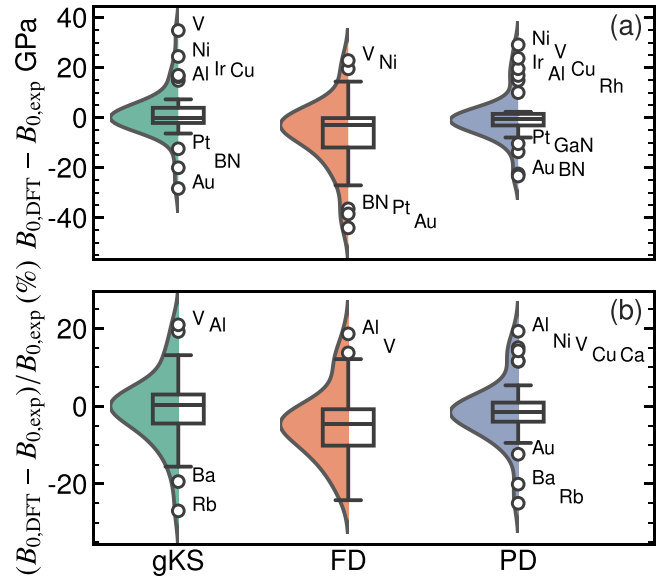

Fig. 2. Visualization (violin plot and box plot) of the deviations from experimental data of the predicted bulk modulus obtained with the different implementations of meta-GGA. See Fig. 1 and main text for details.

Table 1
Calculated Kohn-Sham band gaps in eV for 20 insulators or semiconductors in the test set. PD and FD results are obtained with the Elk code. The gKS results are from Ref. [44]. The last column reports optimized effective potential results from Yang *et al.* Ref. [45] obtained with the Krieger-Li-Iafrate approximation [46].

Solid	Expt.	gKS	FD	PD	KLI (Ref. [45])
C	5.50	—	4.26	4.05	4.26
Si	1.17	0.79	0.74	0.45	0.78
Ge	0.74	0.31	0.14	0.045	—
SiC	2.42	—	1.60	1.30	—
BN	6.36	4.91	4.73	4.34	4.73
BP	2.10	1.47	1.40	1.12	1.52
AlN	4.90	4.95	3.60	3.28	—
AlP	2.50	1.95	1.77	1.43	—
AlAs	2.23	1.81	1.69	1.34	—
GaN	3.28	2.32	1.48	1.76	—
GaP	2.35	1.86	1.60	1.40	1.72
GaAs	1.52	0.96	0.34	0.29	0.45
InP	1.42	—	0.45	0.35	0.77
InAs	0.42	0.09	0.43	0.39	—
InSb	0.24	0.04	0.42	0.35	—
LiH	4.94	—	3.79	2.78	—
LiF	14.20	10.71	9.23	9.02	9.11
LiCl	9.40	7.52	6.55	5.99	—
NaF	11.50	7.44	6.40	6.04	—
NaCl	8.50	6.05	5.40	4.72	5.25

conserving pseudopotentials (missing nonlinear core corrections) in place of the PAW formalism used in VASP [49,50]. The comparison between PD and gKS simulations (third and fourth columns) is instead showing perfect agreement, with the only exceptions being Al and Si.

Magnetic properties, reported in Table 3, are the most sensitive to the choice of the deorbitalization scheme. It has indeed already extensively discussed how gKS leads to overhestimated magnetization in transition metal elements [53,52,54]. On the other hand, FD and PD improve the agreement with experimental results for the elemental ferromagnets Fe, Co and Ni, and also predict the expected non-magnetic ground state for vanadium. These align well also with the recently published Laplacian level OFR2 meta-GGA functional [55].

The density of states for the four elemental solids obtained with LDA and PD is shown in Fig. 3. Small differences in the densities of states of the ground states can be appreciated. The plot shows that, relative to

Table 2
Plane wave results: calculated cohesive energies in eV/atom. MRT data are from Ref. [18] and have been obtained with a different set of pseudopotentials. Experimental values are from Ref. [47,43,48] and references therein.

	Expt.	MRT		This work	
		gKS	FD	gKS	PD
Al	3.43	3.61	3.43	3.82	3.64
Ag	2.96	2.87	2.51	2.86	2.84
Ba	1.91	1.82	1.83	1.87	1.81
Ca	1.87	1.92	1.99	1.99	1.99
Ge	3.89	3.89	3.53	4.15	4.19
Ir	6.99	7.16	6.58	8.06	8.03
Na	1.12	1.04	1.02	1.07	0.99
Pd	3.93	4.17	4.72	4.16	4.11
Rh	5.78	5.49	5.23	5.30	5.30
Si	4.68	4.68	4.50	4.43	4.73

Table 3
Calculated magnetic moment (in μ_B) for a selection of ferromagnets and anti-ferromagnets. gKS results are from Ref. [18] and Ref. [51]. Experimental results are taken from Ref. [52] and references therein.

Solid	Expt.	gKS	FD	PD
Ferromagnets				
Fe	1.98–2.08	2.63	2.27	2.26
Co	1.52–1.62	1.77	1.67	1.61
Ni	0.52–0.55	0.74	0.69	0.60
V	0.00	0.03	0.06	0.0
Anti-ferromagnets				
FeO	3.32–4.6	3.542	3.53	3.44
CoO	3.35–3.98	2.575	2.52	2.43
NiO	1.9–2.2	1.577	1.48	1.27
MnO	4.58	4.446	4.43	4.34

LDA, PD shifts the spin majority occupied states downward, while the spin minority state energies are only slightly increased in all elements but iron, where the effect is more pronounced but only in the conduction bands. The overall effect is very limited and indeed the resulting magnetic moments are very close.

For the anti-ferromagnetic, insulating magnetic oxides FeO, CoO, NiO and MnO the picture is more mixed. The atomic moment of MnO is close to the experimental value and that of FeO lies within the admittedly broad range of measured moments. However, the moments of CoO and NiO are underestimated by both gKS and PD approaches. This has been attributed to strong correlation effects which are not fully described even by meta-GGA functionals.

By calculating the total energy while keeping the moment constrained to a given value (referred to as a fixed spin-moment calculation), it can be ascertained if the self-consistent solution is truly variational. The energy vs. moment for Fe, Co and Ni is plotted in Fig. 4 along with the moment from the corresponding self-consistent solutions. As can be seen, the moments obtained self-consistently are generally smaller than the location of the minima of the curves (these minima precisely match those of Tran *et al.* [52], who used GGA potentials and SCAN total energies). At the energy minimum, the estimates tend to the gKS prediction, not only for magnetic moments, but also for the charge and spin densities (not shown). Notably, the energy difference between the self consistent results and the energy minimum is a rather small fraction (less than 10%) of the magnetic energy (difference between non-spin-polarized and ferromagnetic ground state). This shows that, despite correcting the magnetic moments, the prediction for the magnetic energy remains largely overestimated, a trend evidenced by previous studies on the SCAN functional [52].

This inconsistency also implies that the calculations are not perfectly variational, which in turn implies, unsurprisingly, that the approximate KE functional is inexact. Fully deorbitalized functionals will

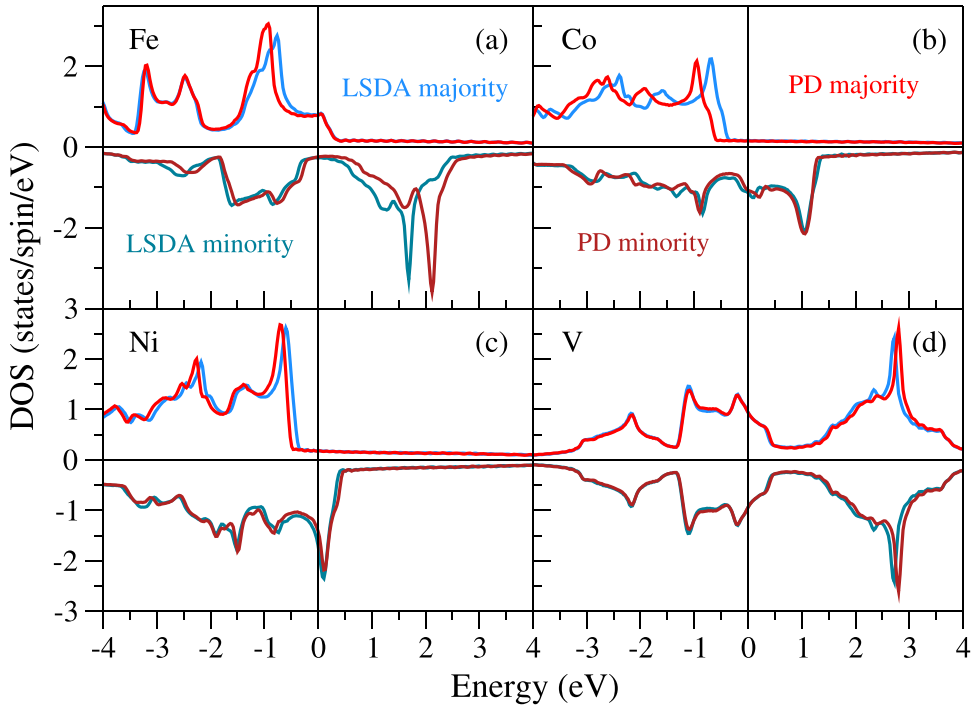

Fig. 3. Spin projected density of states (DOS) in states/spin/eV for (a) Fe (b) Co (c) Ni and (d) V. Results are shown for LDA as well as PD.

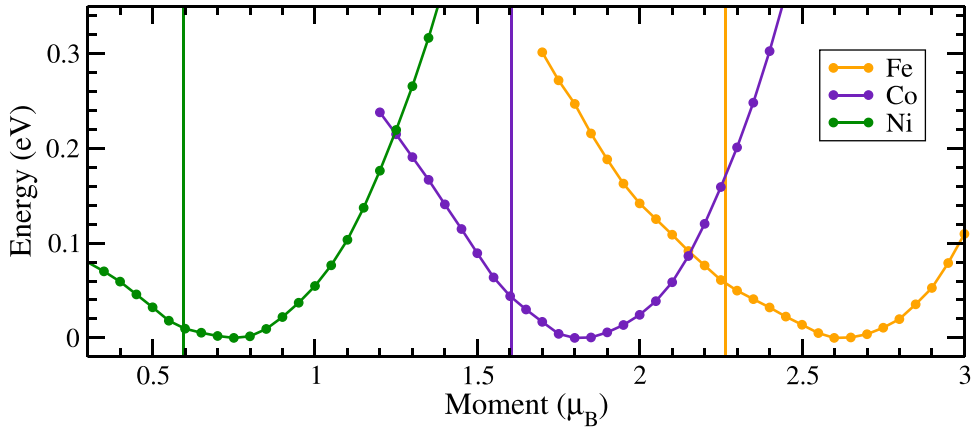

Fig. 4. Energy vs. moment graphs for Fe, Co and Ni using the FP code with PD. The vertical lines indicate the moments obtained self-consistently.

not suffer from this inconsistency because the functional derivative is determined from same KE functional as is used to evaluate the energy (inexact though it is). Nevertheless, this mismatch does serendipitously present us with a useful tool for determining the accuracy of approximate KE functionals: simply check if the solution is at the energy minimum. This is particularly useful because these calculations are for real-world atomistic systems as opposed to simplified models. Magnetic moments can be used as done here, but there are other possibilities: for example testing if the Helmann-Feynman forces on the nuclei are strictly zero at the lowest energy provides an alternative option to confirm that the solution is at the variational minimum.

5. Conclusions

We have modified the deorbitalized approach introduced by MRT by retaining the true Kohn-Sham KE density as input to any meta-GGA exchange-correlation functional, while employing an approximate KE functional for the functional derivative of τ with respect to ρ. This represents a simple route to keeping both E_{xc} inherently non-local and v_{xc} as a local operator in $\mathbf{r}$. DFT codes which already have the gKS version of meta-GGA implemented can be easily modified to accommodate this scheme. We find that even a relatively crude KE functional like TFvW yields results which are, on the whole, at least as accurate as competing approaches such as generalized Kohn-Sham or full deorbitalization. Furthermore, there is ample scope for improvement with respect to both E_{xc} as well as the KE functional. For example, KE functionals involving the Laplacian of the density [28,19] could further enhance the accuracy of method. Showing that the self-consistent solution does indeed correspond to the energy minimum for solids and molecules is a useful measure of the quality of the KE functionals in real-world situations. Lastly, our method may be extended to the case of non-collinear exchange-correlation meta-GGA functionals, at least two of which have been developed recently [56,57]. Treating this type of functional with partial deorbitalization will also require a generalization of the spin-dependent KE density functional to the non-collinear case [58].

Data Availability

Data will be made available on request.

Declaration of Competing Interest

The authors declare that they have no known competing financial interests or personal relationships that could have appeared to influence the work reported in this paper.

Acknowledgements

PB thanks Roberto De Renzi, Andrea Ferretti, Fabrizio Ferrari Ruffino and Pietro Delugas for fruitful discussions and the students of a work-related internship (Italian PCTO activity) Giacomo Bonvicini, Filippo Pedrazzani, Niccolò Lo Re, Alessandro Zanichelli and Giulio Cacciapuoti for analyzing the equation of state of various elements reported in the manuscript. JKD and SS would like to thank the DFG for funding through project-ID 328545488 TRR227 (project A04). SS would like to thank the Leibniz Professorin program for funding.

Appendix A. Supporting information

Supplementary data associated with this article can be found in the online version at doi:10.1016/j.commt.2024.100002.

References

[1] W. Kohn, L.J. Sham, Phys. Rev. 140 (1965) A1133.
[2] P. Hohenberg, W. Kohn, Phys. Rev. 136 (1964) B864.
[3] J.P. Perdew, K. Schmidt, Jacob's ladder of density functional approximations for the exchange-correlation energy, AIP Conf. Proc. 577 (2001) 1–20.
[4] J.P. Perdew, K. Burke, M. Ernzerhof, Generalized gradient approximation made simple, Phys. Rev. Lett. 77 (1996) 3865–3868.
[5] J.P. Perdew, K. Burke, M. Ernzerhof, Perdew, burke, and ernzerhof reply, Phys. Rev. Lett. 80 (1998) 891.
[6] A.D. Becke, On the large-gradient behavior of the density functional exchange energy, J. Chem. Phys. 85 (1986) 7184–7187.
[7] A.D. Becke, M.R. Roussel, Exchange holes in inhomogeneous systems: A coordinate-space model, Phys. Rev. A 39 (1989) 3761–3767.
[8] J. Tao, J.P. Perdew, V.N. Staroverov, G.E. Scuseria, Climbing the Density Functional Ladder: Nonempirical Meta–Generalized Gradient Approximation Designed for Molecules and Solids, Phys. Rev. Lett. 91 (2003) 146401.
[9] A.D. Becke, Hartree-Fock exchange energy of an inhomogeneous electron gas, Int. J. Quantum Chem. 23 (1983) 1915–1922.
[10] J. Sun, A. Ruzsinszky, J.P. Perdew, Strongly Constrained and Appropriately Normed Semilocal Density Functional, Phys. Rev. Lett. 115 (2015) 036402.
[11] J. Sun, R.C. Remsing, Y. Zhang, Z. Sun, A. Ruzsinszky, H. Peng, Z. Yang, A. Paul, U. Waghmare, X. Wu, M.L. Klein, J.P. Perdew, Accurate first-principles structures and energies of diversely bonded systems from an efficient density functional, Nat. Chem. 8 (2016) 831–836.
[12] Z.-h. Yang, H. Peng, J. Sun, J.P. Perdew, More realistic band gaps from meta-generalized gradient approximations: only in a generalized Kohn-Sham scheme, Phys. Rev. B 93 (2016) 205205.
[13] F. Zahariev, S.S. Leang, M.S. Gordon, Functional derivatives of meta-generalized gradient approximation (meta-GGA) type exchange-correlation density functionals, J. Chem. Phys. 138 (2013) 244108.
[14] R. Garrick, A. Natan, T. Gould, L. Kronik, Exact generalized Kohn-Sham theory for hybrid functionals, Phys. Rev. X 10 (2020) 021040.
[15] I. Theophilou, F. Buchholz, F.G. Eich, M. Ruggenthaler, A. Rubio, Kinetic-energy density-functional theory on a lattice, J. Chem. Theory Comput. 14 (2018) 4072–4087.
[16] D. Mejia-Rodriguez, S.B. Trickey, Deorbitalization strategies for meta-generalized-gradient-approximation exchange-correlation functionals, Phys. Rev. A 96 (2017) 052512.
[17] D. Mejia-Rodriguez, S.B. Trickey, Deorbitalized meta-GGA exchange-correlation functionals in solids, Phys. Rev. B 98 (2018) 115161.
[18] D. Mejía-Rodríguez, S.B. Trickey, Meta-GGA performance in solids at almost GGA cost, Phys. Rev. B 102 (2020) 121109.
[19] J.P. Perdew, L.A. Constantin, Laplacian-level density functionals for the kinetic energy density and exchange-correlation energy, Phys. Rev. B 75 (2007) 155109.
[20] M. Filatov, W. Thiel, Exchange-correlation density functional beyond the gradient approximation, Phys. Rev. A 57 (1998) 189–199.
[21] P. de Silva, C. Corminboeuf, Simultaneous Visualization of Covalent and Noncovalent Interactions Using Regions of Density Overlap, J. Chem. Theory Comput. 10 (2014) 3745–3756.
[22] P. de Silva, C. Corminboeuf, Communication: A new class of non-empirical explicit density functionals on the third rung of Jacob's ladder, J. Chem. Phys. 143 (2015) 111105.
[23] W. Yang, Gradient correction in Thomas-Fermi theory, Phys. Rev. A 34 (1986) 4575.
[24] M.G. Medvedev, I.S. Bushmarinov, J. Sun, J.P. Perdew, K.A. Lyssenko, Density functional theory is straying from the path toward the exact functional, Science 355 (2017) 49–52.
[25] P. Blaha, K. Schwarz, F. Tran, R. Laskowski, G.K.H. Madsen, L.D. Marks, WIEN2k: An APW+lo program for calculating the properties of solids, J. Chem. Phys. 152 (2020) 074101.
[26] A.D. Becke, E.R. Johnson, A simple effective potential for exchange, J. Chem. Phys. 124 (2006) 221101.
[27] F. Tran, P. Blaha, Accurate Band Gaps of Semiconductors and Insulators with a Semilocal Exchange-Correlation Potential, Phys. Rev. Lett. 102 (2009) 226401.
[28] G.L. Oliver, J.P. Perdew, Spin-density gradient expansion for the kinetic energy, Phys. Rev. A 20 (1979) 397–403.
[29] J.W. Furness, A.D. Kaplan, J. Ning, J.P. Perdew, J. Sun, Accurate and Numerically Efficient r2SCAN Meta-Generalized Gradient Approximation, J. Phys. Chem. Lett. 11 (2020) 8208–8215.
[30] J.W. Furness, A.D. Kaplan, J. Ning, J.P. Perdew, J. Sun, Correction to "accurate and numerically efficient r2scan meta-generalized gradient approximation, J. Phys. Chem. Lett. 11 (2020) 9248.
[31] G. Kresse, J. Hafner, Ab initio molecular-dynamics simulation of the liquid-metal–amorphous-semiconductor transition in germanium, Phys. Rev. B 49 (1994) 14251–14269.
[32] G. Kresse, J. Furthmüller, Efficient iterative schemes for ab initio total-energy calculations using a plane-wave basis set, Phys. Rev. B 54 (1996) 11169–11186.
[33] G. Kresse, D. Joubert, From ultrasoft pseudopotentials to the projector augmented-wave method, Phys. Rev. B 59 (1999) 1758–1775.
[34] D. Singh, L. Nordstrom, Planewaves, Pseudopotentials, and the LAPW Method, Springer, US, 2006.
[35] The Elk Code.2024 ⟨http://elk.sourceforge.net/⟩.
[36] P. Giannozzi, et al., QUANTUM ESPRESSO: a modular and open-source software project for quantum simulations of materials, J. Phys.: Condens. Matter 21 (2009) 39550219pp.
[37] M. Schlipf, F. Gygi, Optimization algorithm for the generation of ONCV pseudopotentials, Comput. Phys. Commun. 196 (2015) 36–44.
[38] A.B. Alchagirov, J.P. Perdew, J.C. Boettger, R.C. Albers, C. Fiolhais, Energy and pressure versus volume: Equations of state motivated by the stabilized jellium model, Phys. Rev. B 63 (2001) 224115.
[39] M.L. Waskom, seaborn: statistical data visualization, J. Open Source Softw. 6 (2021) 3021.
[40] L. Schimka, R. Gaudoin, J.C.V. Klimeš, M. Marsman, G. Kresse, Lattice constants and cohesive energies of alkali, alkaline-earth, and transition metals: Random phase approximation and density functional theory results, Phys. Rev. B 87 (2013) 214102.
[41] P. Kovács, F. Tran, P. Blaha, G.K.H. Madsen, Comparative study of the PBE and SCAN functionals: The particular case of alkali metals, J. Chem. Phys. 150 (2019) 164119.
[42] P. Haas, F. Tran, P. Blaha, Calculation of the lattice constant of solids with semilocal functionals, Phys. Rev. B 79 (2009) 085104.
[43] F. Tran, J. Stelzl, P. Blaha, Rungs 1 to 4 of DFT Jacob's ladder: Extensive test on the lattice constant, bulk modulus, and cohesive energy of solids, J. Chem. Phys. 144 (2016) 204120.
[44] M. Kothakonda, A.D. Kaplan, E.B. Isaacs, C.J. Bartel, J.W. Furness, J. Ning, C. Wolverton, J.P. Perdew, J. Sun, Testing the r2SCAN Density Functional for the Thermodynamic Stability of Solids with and without a van der Waals Correction, ACS Mater. Au 3 (2023) 102–111.
[45] Z.-h. Yang, H. Peng, J. Sun, J.P. Perdew, More realistic band gaps from meta-generalized gradient approximations: Only in a generalized Kohn-Sham scheme, Phys. Rev. B 93 (2016) 205205.
[46] J.B. Krieger, Y. Li, G.J. Iafrate, Construction and application of an accurate local spin-polarized Kohn-Sham potential with integer discontinuity: Exchange-only theory, Phys. Rev. A 45 (1992) 101–126.
[47] H. Peng, Z.-H. Yang, J.P. Perdew, J. Sun, Versatile van der Waals Density Functional Based on a Meta-Generalized Gradient Approximation, Phys. Rev. X 6 (2016) 041005.
[48] C. Kittel, Introduction to Solid State Physics, Wiley, 1996.
[49] E.B. Isaacs, C. Wolverton, Performance of the strongly constrained and appropriately normed density functional for solid-state materials, Phys. Rev. Mater. 2 (2018) 063801.
[50] Y. Yao, Y. Kanai, Plane-wave pseudopotential implementation and performance of SCAN meta-GGA exchange-correlation functional for extended systems, J. Chem. Phys. 146 (2017) 224105.
[51] S. Swathilakshmi, R. Devi, G. Sai Gautam, Performance of the r2SCAN Functional in Transition Metal Oxides, J. Chem. Theory Comput. 19 (2023) 4202–4215 PMID: 37329316.
[52] F. Tran, G. Baudesson, J. Carrete, G.K.H. Madsen, P. Blaha, K. Schwarz, D.J. Singh, Shortcomings of meta-GGA functionals when describing magnetism, Phys. Rev. B 102 (2020) 024407.
[53] D. Mejía-Rodríguez, S.B. Trickey, Analysis of over-magnetization of elemental transition metal solids from the SCAN density functional, Phys. Rev. B 100 (2019) 041113.
[54] Y. Fu, D.J. Singh, Density functional methods for the magnetism of transition metals: SCAN in relation to other functionals, Phys. Rev. B 100 (2019) 045126.
[55] A.D. Kaplan, J.P. Perdew, Laplacian-level meta-generalized gradient approximation for solid and liquid metals, Phys. Rev. Mater. 6 (2022) 083803.
[56] Z. Pu, H. Li, N. Zhang, H. Jiang, Y. Gao, Y. Xiao, Q. Sun, Y. Zhang, S. Shao, Noncollinear density functional theory, Phys. Rev. Res 5 (2023) 013036.
[57] Tancogne-Dejean, N.; Rubio, A.; Ullrich, C.A. Exchange torque in noncollinear spin density functional theory with a semilocal exchange functional.2022; ⟨https://arxiv.org/abs/2208.07729⟩.
[58] E.I. Tellgren, Universal lower bounds on the kinetic energy of electronic systems with noncollinear magnetism, Phys. Rev. A 97 (2018) 022513.